

1 Compound winter low wind and cold events impacting the French  
2 electricity system: observed evolution and role of large-scale  
3 circulation

4  
5 François Collet<sup>1</sup>, Margot Bador<sup>1</sup>, Julien Boé<sup>1</sup>, Laurent Dubus<sup>2,3</sup>, Bénédicte Jourdièr<sup>2</sup>

7 <sup>1</sup>CECI Université de Toulouse, CERFACS/CNRS, Toulouse, France

8 <sup>2</sup>RTE, Paris, [France](#)

9 <sup>3</sup>[World Energy & Meteorology Council, Norwich, UK](#)

11 Correspondence to : François Collet ([collet@cerfacs.fr](mailto:collet@cerfacs.fr))

a supprimé: a

13 **Abstract.** To reach climate mitigation goals, the share of wind power in the electricity production is  
14 going to increase substantially in France. In winter, low wind days are challenging for the electricity system  
15 if compounded with cold days that are associated with peak electricity demand. The scope of this study is to  
16 characterize the evolution of compound low wind and cold events in winter over the 1950-2022 period in  
17 France. Compound events are identified at the daily scale using a bottom-up approach based on two indices  
18 that are relevant to the French energy sector, derived from temperature and wind observations. The frequency  
19 of compound events shows high interannual variability, with some winters having no event and others having  
20 up to 13. Over the 1950-2022 period, the frequency of compound events has decreased, which is likely due to  
21 a decrease in the frequency of cold days. Based on a k-means unsupervised classification technique, four  
22 weather types are identified, highlighting the diversity of synoptic situations leading to the occurrence of  
23 compound events. The weather type associated with the highest frequency of compound events presents  
24 pronounced positive mean sea-level pressure anomalies over Iceland and negative anomalies west of Portugal,  
25 limiting the entrance of the westerlies and inducing a north-easterly flow bringing cold air over France and  
26 Europe generally. We further show that the atmospheric circulation and its internal variability are likely to  
27 play a role in the observed reduction in cold days, suggesting that this negative trend may not be entirely be  
28 driven by anthropogenic forcings. It is however more difficult to conclude on the role of the atmospheric  
29 circulation in the observed decrease in compound events.

a supprimé: and a decrease over the 1950-2022 period.

a supprimé: Despite this suggested role for cold days, the observed decrease in compound events does not seem to be strongly influenced by the regional atmospheric circulation

31 **1 Introduction**

37 The transition of the energy system, including the reinforced integration of renewable energy, is  
38 necessary to reduce greenhouse gas emissions in accordance with the Paris Agreement. A recent report from  
39 the French electricity transmission system operator (Réseau de Transport d'électricité, 2023 ; RTE in the  
40 following) shows that the national energy transition will rely on a widespread electrification of residential  
41 heating, transport, and the industry, along with improving energy efficiency (e.g., thermal renovation of  
42 buildings). Therefore, the electricity demand is projected to increase from 475TWh in 2019 to 580-640 TWh  
43 in 2035, according to scenarios in which France meets its energy transition goals (see scenarios A in RTE,  
44 2023). In light of the future electricity demand, France has expressed its intention to significantly expand its  
45 wind energy capacity in the coming decades. Onshore wind power capacity is planned to increase from 20GW  
46 in 2022 to 30-39GW by 2035 and substantial additional offshore wind farms are also planned, with a total  
47 projected capacity of 18GW by 2035 compared to 0.5GW in 2022 (RTE, 2023).

48 The production and demand of electricity can be affected by a range of climate conditions over multiple  
49 time scales. In terms of electricity demand during winter, France is known to be one of the most temperature  
50 sensitive among European countries (Bloomfield et al., 2020a). This is mainly explained by the high usage of  
51 electricity for residential heating, which is expected to increase over the next decades (RTE, 2023). Hence,  
52 cold events will likely continue being associated with peak electricity demand based on the projections of the  
53 French future electricity system (RTE, 2023). Besides, part of the electricity production in France relies on  
54 renewable energies that are sensitive to climate conditions including wind speed, solar radiations, and river  
55 flows. As the proportion of renewable energy in the French electricity mix is set to rise, the electricity  
56 production will be more importantly affected by climate variability. In particular, it is anticipated that a higher  
57 proportion of wind power in the electricity mix may lead to higher risks for the production of electricity,  
58 especially during low wind events. This is particularly the case in winter, when solar generation represents a  
59 smaller share of the electricity production (Grams et al., 2017; Otero et al., 2022b). Hence, in France, it can  
60 be challenging to ensure adequate electricity supply and demand due to the occurrence of multivariate  
61 compound events (Zscheischler et al., 2020), such as low wind and cold events, which can create stressful  
62 situations. The aim of this study is to characterize compound low wind and cold events in France.

63 Overall, there is little information in the literature on the observed evolution of compound low wind  
64 and cold events in France and Europe. A body of studies focuses on related events using electricity supply and  
65 production data. For instance, an electricity supply drought is defined by a sequence of days with low  
66 renewable electricity production and high electricity demand (Raynaud et al., 2018). Most of these studies  
67 focus on the characterization of the statistical properties of these events (Otero et al., 2022a, b; Raynaud et al.,  
68 2018; Tedesco et al., 2023) or their drivers (Bloomfield et al., 2020a; Ravestein et al., 2018; Thornton et al.,  
69 2017; van der Wiel et al., 2019a, b). Only a limited number of these studies focus on their temporal evolution  
70 in the context of climate change. Van der Wiel et al. (2019a) show that the frequency of electricity supply  
71 droughts in Europe is reduced in a 2°C warmer world compared to present day conditions, using projections  
72 from two global climate models. Although there is a gap in the understanding of the past evolution of

a supprimé: projected

74 compound low wind and cold events, changes in low wind or cold events have been investigated  
75 independently. Rapella et al. (2023) showed that the number of low wind events decreases in the ERA5  
76 reanalysis over the 1950-2022 period. However, they focus only on offshore regions such as the Bay of Biscay,  
77 the North Sea, and the Channel, in summer and at the annual scale. Focusing on cold temperature conditions  
78 in winter, there is evidence that the frequency and intensity of cold spells have decreased over the last decades  
79 in Europe (Cattiaux et al., 2010; Seneviratne et al., 2021; Van Oldenborgh et al., 2019). While there is clear  
80 evidence that climate change leads to a reduction in cold events, there are still major uncertainties regarding  
81 low wind events. It is therefore difficult to anticipate how compound low wind and cold events may change  
82 in the coming decades as there is a lack of understanding of their past evolution. An objective of this study is  
83 to assess the evolution of these compound events in the observational record.

84 This work also focuses on the influence of the large-scale atmospheric circulation on the occurrence  
85 and evolution of compound low wind and cold events. The atmospheric circulation is an important driver of  
86 temperature variability (Plaut and Simonnet, 2001) and wind speed variability (Najac et al., 2009) in France,  
87 and here we aim to further assess its influence on compound events in winter. In the literature, different  
88 approaches have been used to explore the influence of the atmospheric circulation and its variability in  
89 favoring particular meteorological situations that affect the electricity sector. This includes identifying weather  
90 regimes of interest (Otero et al., 2022b; van der Wiel et al., 2019b; Tedesco et al., 2023), targeted circulation  
91 types (Bloomfield et al., 2020b), and circulation regimes based on large-scale conditions leading to critical  
92 situations for the electricity system such as days with extremely high electricity demand (Thornton et al.,  
93 2017).

94 Finally, we investigate to what extent the large-scale atmospheric circulation and its variability  
95 contribute to the past evolution of compound low wind and cold events in France. Several studies found that  
96 recent changes in the large-scale circulation play a role in the winter trend in mean temperature across Europe  
97 (Deser and Phillips, 2023; Sippel et al., 2020; Saffioti et al., 2016), and in the decreasing occurrence and  
98 intensity of cold extremes (Horton et al., 2015; Terray, 2021). Using a dynamical adjustment approach based  
99 on observations (Terray, 2021), we explore the role of the changes in atmospheric circulation in the observed  
100 trend in compound low wind and cold events in France.

101 This paper is organized as follows: section 2 presents the data and the method used, section 3 presents  
102 the main results and section 4 includes a conclusion and discussion of the findings.

## 103 2 Data and Method

104 In this study, we identify compound low wind and cold events based on a wind capacity factor index  
105 and a temperature index. These indices respectively capture the sensitivity of the French wind power  
106 production to wind speed conditions and the sensitivity of the French electricity demand to temperature  
107 conditions. Thus, compound events as defined in this study correspond to days when the French power system  
108 is challenged by both wind and temperature conditions. In this section, we first introduce the data and

a supprimé: regional

a supprimé: Tedesco et al. (2023) showed that compound low wind and cold events in France are mostly associated with positive anomalies of geopotential height at 500hPa over Iceland and negative anomalies over the Azores. Otero et al. (2022b) showed that situations of limited production of electricity from wind and solar energies co-occurring with cold events are mostly associated with positive anomalies of geopotential height at 500hPa over the North Sea region.

a supprimé: regional

a supprimé: data

120 methodology used to define the wind capacity factor and temperature indices. Then, we introduce the  
121 methodology used to identify compound low wind and cold events. Finally, methodologies used to identify  
122 weather types and to assess the role of the atmospheric circulation in the evolution of compound events are  
123 developed,

## 124 2.1 Observations and reanalyses of atmospheric variables

125 The ERA5 reanalysis data (Hersbach et al., 2020) is used over the period 1950-2022. ERA5 is available  
126 on a regular grid with a resolution of about 30 km in Europe. In particular, the hourly wind speed (at 100 m)  
127 and the daily near-surface air temperature (at 2 m) are used for the calculation of the wind capacity factor and  
128 temperature indices, respectively (section 2.3 and 2.4). Daily mean sea level pressure is also used for  
129 classification of the large-scale circulation into weather types (see section 2.6) and dynamical adjustment  
130 (section 2.7). In addition to the ERA5 reanalysis, wind and temperature data from the MERRA-2 reanalysis  
131 (Gelaro et al., 2017) are considered. MERRA-2 is available at a horizontal resolution of about 60 km over  
132 Europe, over the 1980-2022 period. Hourly near-surface air temperature and wind (at 50 m) are used. We also  
133 consider in situ temperature observations from the gridded E-OBS dataset (Comes et al., 2018) over the 1950-  
134 2022 period, available on a regular grid with a horizontal resolution of about 30 km in Europe.

135 This study is mainly focused on an extended winter period, from November to March, when compound  
136 low wind and cold events occur in France. By convention, hereafter, winter 1951 corresponds to the period  
137 from November 1950 to February 1951 and so on,

## 138 2.2 Observations of the wind power production and electricity demand in France

139 Hourly observed data for the wind power production and electricity demand in France are taken from the  
140 éCO2mix dataset ([https://odre.opendatasoft.com/explore/dataset/eco2mix-national-cons-  
141 def/information/?disjunctive=nature](https://odre.opendatasoft.com/explore/dataset/eco2mix-national-cons-def/information/?disjunctive=nature)), over the 2012-2020 period. The French wind power installed capacity is  
142 available at 3-monthly time intervals over the 2012-2020 period at [https://www.statistiques.developpement-  
143 durable.gouv.fr/publicationweb/549](https://www.statistiques.developpement-durable.gouv.fr/publicationweb/549). Hourly observed wind capacity factor is calculated using the hourly  
144 observed wind power production from éCO2mix, which is divided by the wind power installed capacity in  
145 France of the corresponding 3-monthly interval.

## 146 2.3 Wind capacity factor index

a supprimé: First, the data and the methodology used to identify low wind events, cold events, and compound low wind and cold events responsible for stressful situations for the adequacy between electricity demand and supply in France are described.

a supprimé: e

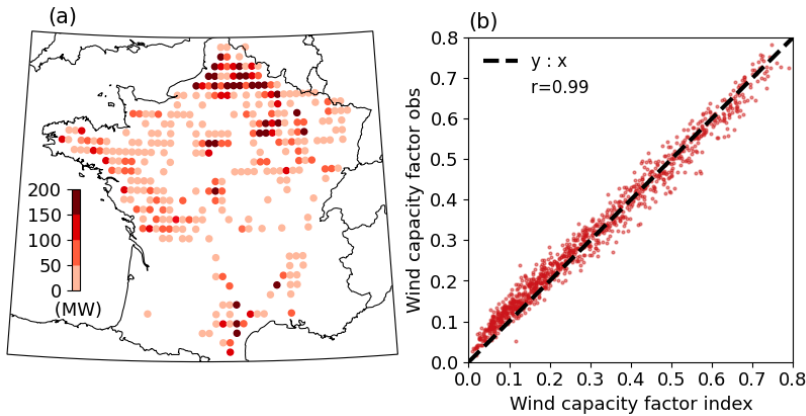


Figure 1: (a) Spatial distribution of the wind power installed capacity (MW) in France in 2021 from the WindPower.net dataset used for the calculation of the wind capacity factor index. (b) National French wind capacity factor index as calculated with ERA5 (no unit; X-axis) versus observations (no unit; Y-axis) in winter over the 2012-2020 period. The correlation coefficient is given in the top left corner, and the black dashed line represents the  $y:x$  function.

Several studies (Bloomfield et al., 2022; Jourdier, 2020; Olauson, 2018; Staffell and Pfenninger, 2016) demonstrated that it is possible to calculate hourly wind capacity factor at country-scale with a good accuracy using wind speed from reanalysis data in Europe. Here, we use a similar approach to calculate the French wind capacity factor index over the 1951-2022 period.

This approach requires information at each wind farm site, which are taken from The Wind Power database (<https://www.thewindpower.net/>), including the location, rated power, hub height, and power curves at each site (upon availability). Only wind farms operational in 2021 are used (i.e., those with “in production” status). This represents a total number of 1661 wind farms and a total installed capacity of 19GW. Wind farms and related wind power installed capacity are concentrated in the North-East of France (Figure 1a). While the installed wind power capacity is fairly accounted for in this database, there is a substantial amount of missing data regarding the hub heights and the power curves (~29% and ~7% of wind farms, respectively). Missing data is filled in following the methodology introduced in Jourdier (2020), which broadly consists in taking characteristics from wind farms identified as similar in terms of rated power, rated diameter, rated wind speed, cut-in and cut-off wind speed.

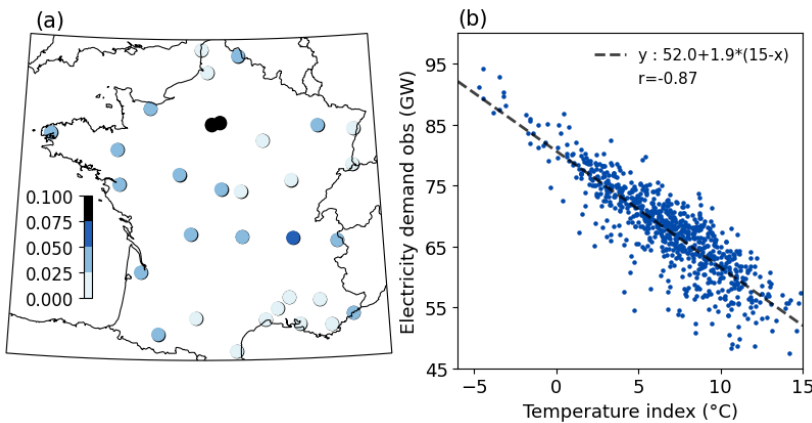
To calculate the wind capacity factor, ERA5 hourly wind speeds at 100 m are first interpolated to each wind farm site using a nearest neighbor interpolation scheme. The wind speeds are then extrapolated at hub height using a power law ( $\alpha=0.14$ ; Manwell, 2010; van der Wiel et al., 2019a). Then, using the power curve of each wind farm, wind speed at the hub height is converted into power production. Finally, the hourly wind capacity factor over France is estimated by summing the power production from all wind farms, and dividing

**a supprimé:** Calculation of the wind capacity factor first requires interpolating ERA5 hourly wind speed from 100 m at each wind farm’s hub height. This is done using a power law ( $\alpha=0.14$ ; Manwell, 2010; van der Wiel et al., 2019a)

183 this total power production by the total installed capacity. Finally, hourly wind capacity factors are averaged  
184 to daily values to further identify low wind days (section 2.5).

185 The daily wind capacity factor index computed with this approach is extremely well correlated with  
186 observations over their 9 common winters ( $r=0.99$ , Figure 1b), highlighting the relevance of using ERA5 data  
187 in this context.

## 188 2.4 Temperature index representative of the demand in electricity



189  
190 **Figure 2: (a) Location of the 32 French cities and associated weights (no unit) used for the calculation**  
191 **of the temperature index. (b) Temperature index as calculated in ERA5 (°C; X-axis) versus observations of**  
192 **the electricity demand (GW; Y-axis) in winter over the 2012-2020 period, excluding week-ends and bank**  
193 **holidays. The correlation coefficient is given in the top right corner. The linear regression line between the**  
194 **temperature index and the electricity demand observations is shown by the black dashed line. The**  
195 **corresponding linear regression equation, in the form  $y=y(15^{\circ}\text{C})+a*(15^{\circ}\text{C}-x)$ , where  $15^{\circ}\text{C}$  is the threshold of**  
196 **residential heating and a the thermosensitivity of the electricity demand, is shown in the top right corner.**

198 The temperature index is defined following an approach used operationally by RTE that consists in  
199 calculating a weighted average of temperature data from 32 cities in France (Figure 2a), which is  
200 representative of the electricity demand in France. First, the near-surface air temperature in ERA5 at the grid-  
201 cell closest to each city location is selected. Then, temperatures are corrected based on the difference between  
202 the elevation of the grid cell and the elevation of the in situ station for each city, assuming a vertical gradient  
203 of temperature of  $-6.5^{\circ}\text{C}/\text{km}$ . Finally, the weighted average of temperature at the 32 locations is calculated  
204 over the 1950-2022 period.

205 A strong anti-correlation of  $-0.87$  is found between the temperature index and the observed electricity  
206 demand in winter (Figure 2b). This highlights the relevance of the temperature index as a proxy for the French  
207 demand in electricity.

a supprimé: 2a

a supprimé: 1.b

a supprimé: 2

a supprimé: Figure 2: (a) National French wind capacity factor index as calculated with ERA5 (no unit; X-axis) versus observations (no unit; Y-axis) in winter over the 2012-2020 period. The correlation coefficient is given in the top left corner, and the black dotted line represents the y:x function. (b) Temperature index as calculated in ERA5 (°C; X-axis) versus observations of the electricity demand (GW; Y-axis) in winter over the 2012-2020 period, excluding week-ends and bank holidays. The correlation coefficient is given in the top right corner. The linear regression line between the temperature index and the electricity demand observations is shown by the black dashed line. The corresponding linear regression equation, in the form  $y=y(15^{\circ}\text{C})+a*(15^{\circ}\text{C}-x)$ , where  $15^{\circ}\text{C}$  is the threshold of residential heating and a the thermosensitivity of the electricity demand, is shown in the top right corner.

## 2.5 Identification of low wind days, cold days and associated compound events

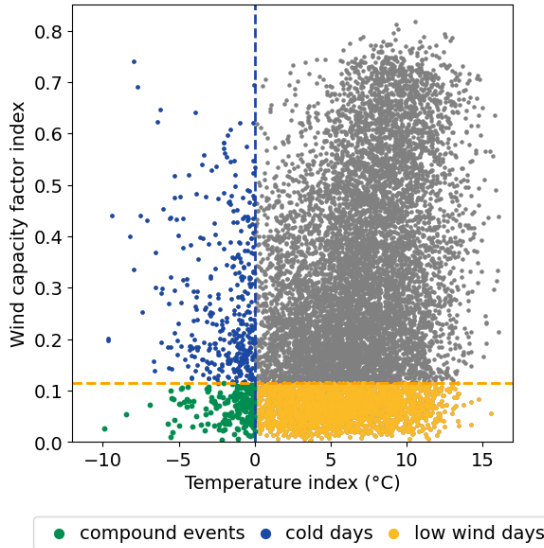
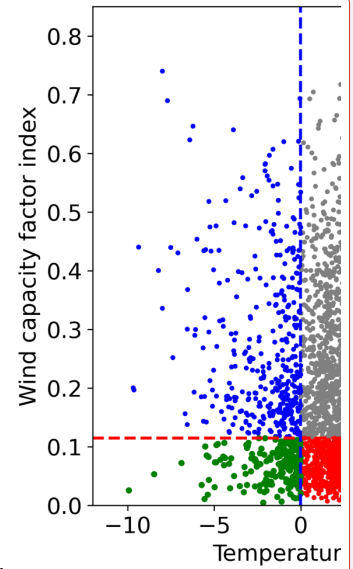


Figure 3: Wind capacity factor index (no units; Y-axis) and temperature index (°C; X-axis) calculated with ERA5 for each winter day over the 1951-2022 period. Yellow and blue dashed lines show the thresholds used to identify low wind days and cold days (yellow and blue points, respectively). Compound low wind and cold events are identified by the green dots.

In this study, compound events are defined as days when low wind capacity factor and cold temperature co-occur (green points in Figure 3). Days of low wind capacity factor (yellow points in Figure 3) are defined as days with an observed wind capacity factor below 0.15, corresponding to the 23th percentile of its distribution in winter. This sample of low wind capacity factor days only captures days with low values of 100-m wind speed over France (see Figure S1). Thus, these events are referred to as low wind days. Cold days are defined as days with the temperature index below 0°C, corresponding to the 5th percentile of its distribution in winter (blue points in Figure 3). In this study, we chose to set a more extreme threshold for the temperature index compared to the wind capacity factor index because risks to the French power system have historically been primarily related to the occurrence of cold waves in winter (Añel, 2017). However, depending on future levels of wind power installed capacity and demand patterns, the sensitivity of the power system to these thresholds might change. Sensitivity tests exploring different thresholds for both indices are therefore included in Supplementary Materials. These tests show limited sensitivity to thresholds for the definition of compound events, except for the long-term trend in the observed occurrence of compound events over the 1951-2022 period.

## 2.6 Weather types of low wind days

a supprimé: -



a supprimé:

a supprimé: Red

a supprimé: red

a supprimé: In this study, compound low wind and cold events are defined as days when cold temperature and low wind conditions co-occur (green points in Figure 3). Cold days are defined here as days with the temperature index below 0°C, corresponding to the 5th percentile of the distribution of the temperature index in winter (blue points in Figure 3). Low wind days (red points in Figure 3) are defined as days with a wind capacity factor index below a certain threshold (here the 23th percentile), which corresponds to a wind capacity factor of 0.15 in the distribution of observations in winter.

a supprimé: Classification into weather types

265 A classification of mean sea-level pressure fields on low wind days (i.e., low wind capacity factor day)  
267 is conducted using the k-means unsupervised classification method (e.g., Cassou, 2008; Falkena et al., 2020).  
268 This allows classifying daily synoptic conditions into different large-scale atmospheric circulation types, or  
269 weather types. Here, low wind days solely are considered for the classification instead of compound low wind  
270 and cold events because the corresponding sample size is larger (2549 days compared to 182 days,  
271 respectively; see Figure 3, Figure 4b, and further discussions in section 3). In other words, the weather types  
272 represent clusters of low wind days with similar large-scale circulation patterns. In a second phase, we examine  
273 how cold days are distributed across these different weather types. Finally, we can thus assess the number of  
274 compound event days for each identified weather type.

275 This classification algorithm is first applied repeatedly for different domains and number of clusters.  
276 The objective is to minimize locally the ratio of intra-type to inter-type variance of the temperature index,  
277 while keeping a reasonable number of weather types. Thanks to this procedure, the classification of low wind  
278 days that allows for the best differentiation of the temperature index is chosen. This procedure leads to a  
279 domain whose limits are [30°W-30°E/33°S-70°N], which covers the North-Western Europe region, and a total  
280 number of four clusters.

## 281 2.7 Dynamical adjustment

282 The main objective of dynamical adjustment is to derive an estimate of the contribution of atmospheric  
283 circulation to the variations of a variable of interest (Terray, 2021; Deser et al., 2016; Sippel et al., 2019). In  
284 this study, we use dynamical adjustment to estimate the contribution of atmospheric circulation to the  
285 variations of cold days, low wind days, and compound events.

286 First, we estimate the contribution of atmospheric circulation to the wind capacity factor and  
287 temperature indices, hereafter referred to as their dynamic component. To that purpose, the constructed  
288 analogue approach is used (Terray, 2021; Boé et al., 2023; Deser et al., 2016). Following Lorenz (1969),  
289 analogues are defined as days with very similar atmospheric circulation. As finding genuinely good analogues  
290 in a finite database could be difficult, synthetic analogues can be constructed through the linear combination  
291 of the atmospheric circulation corresponding to a large number of more or less good analogues (Van Den  
292 Dool, 1994).

293 First, for each target day of the winters 1951-2022, the 400 closest analogues are searched in winter  
294 using the Euclidean distance calculated with ERA5 mean sea-level pressure interpolated on a 2°x2° grid on  
295 the North-Western Europe domain (section 2.6). The winter of the target day is excluded from the search pool.  
296 Then for each target day, a subset of 200 analogues are randomly selected from the 400 analogues, and the  
297 optimal linear combination of this subset of 200 analogues that best matches the mean sea level pressure of  
298 the target day is calculated. This allows obtaining a constructed analogue for the target day. This procedure is  
299 repeated 200 times, to obtain 200 constructed analogues for each target day and the corresponding 200 sets of  
300 optimal weights. While the 200 constructed analogues of each target day have very similar atmospheric

a supprimé: However, in a second phase, we assess how cold days and therefore compound events are distributed across the different weather types leading to low wind days

a supprimé: Hereafter, the contribution of atmospheric circulation is referred to as the dynamic component.

a supprimé: dynamic component of

a supprimé: 1500

a supprimé: 1300

a supprimé: 1500

a supprimé: 1300

a supprimé: 50

a supprimé: 50

a supprimé: 50

a supprimé: 50



circulation to the target day, this procedure, together with the large number of analogues used allows us to sample different land surface and ocean conditions that might otherwise influence the estimate of the dynamic components (Terry, 2021).

For each target day, the wind capacity factor and the temperature indices are then reconstructed by applying the same set of optimal linear weights to the corresponding wind capacity factor index and detrended anomalies of the temperature index, respectively. There are 200 reconstructions of the wind capacity factor and the temperature index per day over the winters 1951-2022. As we are interested in separating the trend due to large-scale circulation from thermodynamically-forced changes, an estimate of the forced trend of the temperature index anomaly for each winter month is removed before applying the dynamical adjustment. This low-frequency trend is estimated using a low-frequency LOESS smoother as done in Terry (2021). Finally, a best estimate of the dynamic component of the wind capacity factor index and the temperature index are derived by averaging the 200 reconstructions of the wind capacity factor index and the temperature index, respectively.

To isolate the impact of large-scale circulation on the evolution of compound events, we define circulation-induced compound events. These are virtual events based only on the contribution of large-scale circulation. First, circulation-induced low wind days and cold days are identified using the same thresholds as for the definition of low wind days and cold days (i.e., the 5th percentile and the 23rd percentile of the extended winter distribution, respectively; Section 2.5), but this time on the dynamic component of the wind capacity factor and temperature indices, respectively. Finally, circulation-induced compound events are identified as days when both the circulation-induced low wind days and circulation-induced cold days virtually occur.

### 3. Results

#### 3.1 Climatological characteristics and observed evolution of compound low wind and cold events

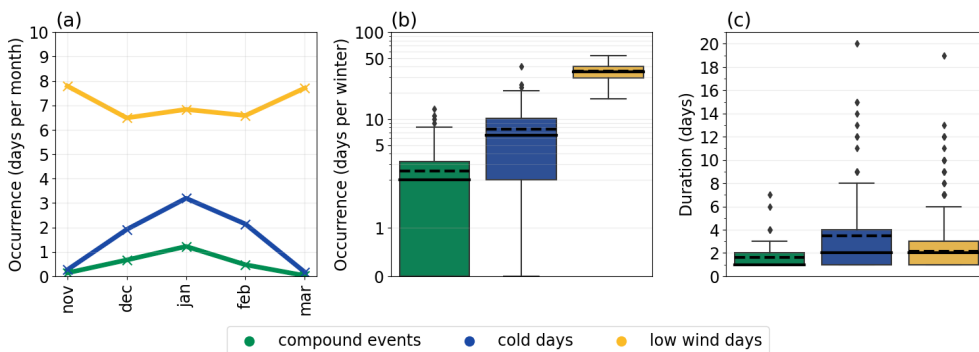


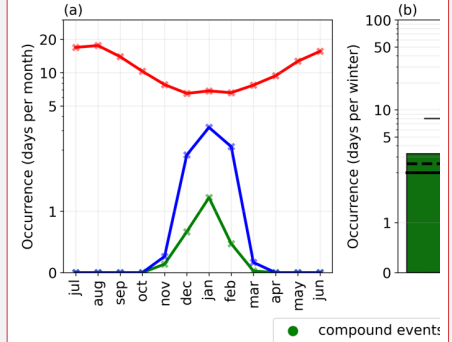
Figure 4: (a) Monthly mean number of compound low wind and cold events (green), cold days (blue), and low wind days (yellow); Distributions of (b) the number of days per winter and (c) duration of compound low wind and cold events, cold days, and low wind days in winter over the 1951-2022 period in ERA5. The solid line and the dashed line in the boxplots in (b) and (c) show the median and the average, respectively.

a supprimé: 50

a supprimé: 50

a supprimé: Finally, the dynamic component of low wind days and cold days is defined using the same thresholds as for the definition of cold days and low wind days (i.e., the 5th percentile and the 23th percentile, respectively; section 2.5). This allows the dynamic component of compound events to be identified as days when both the dynamic component of low wind days and cold days occur.

a supprimé: 4

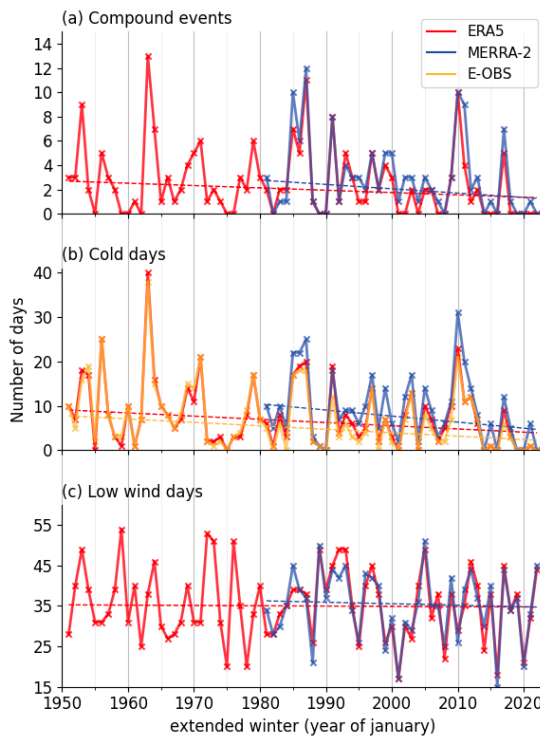


a supprimé: red

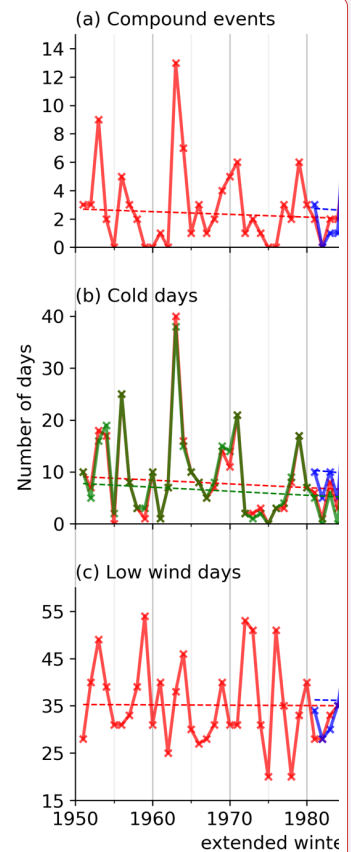
354  
 355 During the extended winter period (November to March), there are clear monthly variations in the  
 356 occurrence of compound events, which are concentrated in mid-winter months (i.e., December to February)  
 357 and peak in January (Figure 4a). This is well explained by cold days that have similar monthly variations,  
 358 while low wind days (i.e., days with low wind capacity factor) predominantly occur during early and late  
 359 winter months (i.e., November and March).

360 The median number of compound events per winter (2 days; Figure 4b) is a third of the median number  
 361 of cold days per winter (6 days; Figure 4b). The median number of low wind days per winter reaches 35 days,  
 362 and is therefore substantially higher than for compound events and cold days. In terms of year-to-year  
 363 variability, we find that the number of compound events ranges from 0 to 13 days per winter, while there are  
 364 from 0 to 40 cold days and 17 to 54 low wind days. When compared to the mean, the interannual variability  
 365 is thus higher for the occurrence of compound events and cold days compared to low wind days.

366 On average in winter, the duration of compound events is estimated to be around 2 consecutive days, 3  
 367 days for cold days and 2 days for low wind days (Figure 4c). The maximum duration of compound events is  
 368 7 consecutive days, corresponding to the period between 17 and 23 January 1987, at the end of a severe 13-  
 369 day cold spell. Overall, compound low wind and cold events are relatively rare and generally short-lived, but  
 370 they can last for a few days and up to a week occasionally.



a supprimé: There is a clear seasonality in the occurrence of compound events, which are concentrated in winter (November to March; Figure 4a). This is well explained by the seasonality of cold days, which occur from November to March in France. Conversely, low wind days are less frequent in winter, with an average of 7 days for winter months compared to an average of 13 days for other months.



a supprimé:

380 Figure 5: Interannual evolution of the number of (a) compound low wind and cold events, (b) cold days, (c)  
 381 and low wind days per winter in ERA5 (in red; 1951-2022), MERRA2 (in blue; 1981-2022) and EOBS (in  
 382 yellow; 1951-2022) datasets. Dashed lines show the linear trend (calculated with the Theil-Sen estimator; see  
 383 Table 1 for the slope value and associated significance).

Data	ERA5		MERRA-2		E-OBS	
	1951-2022	1981-2022	1951-2022	1981-2022	1951-2022	1981-2022
Compound events	<b>-0.19 (0.02)</b>	<b>-0.43 (0.01)</b>	/	-0.36 (0.1)	/	/
Cold days	<b>-0.72 (0.02)</b>	-1.03 (0.08)	/	-1.36 (0.08)	<b>-0.78 (0.0)</b>	-0.67 (0.16)
Low wind days	-0.08 (0.59)	-0.45 (0.48)	/	-0.37 (0.72)	/	/

385 Table 1: Trend (slope in days/decade) and associated p-value, in the number of compound low wind and cold  
 386 events, cold days, and low wind days in ERA5, MERRA-2 and E-OBS over their respective time period (as  
 387 indicated in the first row). The slope is calculated with Theil-Sen estimator and the p-value with the Mann-  
 388 Kendall test. Significant trends with  $p < 0.05$  are shown in bold. Cells with « / » correspond to missing data.

389 Further looking into the year-to-year differences in the number of compound low wind and cold events,  
 390 we find substantial interannual variability (Figure 5a). Some winters stand out as extreme cases, such as 1963,  
 391 1985, 1987, and 2010. In particular, the exceptional winter 1963, is the most extreme winter with 13 days of  
 392 compound events (Figure 5b). Winter 1963 is the coldest winter ever recorded over Western Europe (Hirschi  
 393 and Sinha, 2007) and our results further show that low wind days were co-occurring with some of these cold  
 394 days. Overall, there is a good agreement between ERA5 and MERRA-2 over the shorter 1981-2022 period.  
 395 This includes the characterization of the most extreme winters in terms of compound events, although  
 396 MERRA2 generally shows a slightly higher number of compound events per winter.

397 The interannual variability of compound events is primarily driven by the variability of cold days  
 398 compared to the variability of low wind days ( $r=0.86$  and  $r=0.19$  in ERA5, respectively; Figure 5a,b). In  
 399 particular, the highest numbers of compound events are found in years also characterized by the highest  
 400 numbers of cold days, but not necessarily in years with the highest numbers of low wind days (e.g., 1963,  
 401 1987, 2010, Figure 5a,b,c). This is due to the more extreme threshold applied on the temperature index and  
 402 therefore the larger sample of low wind days per winter on average compared to the number of cold days  
 403 (section 2.5 and sensitivity analyses in Supplementary Material).

404 Over the 1951-2022 period, there is a significant decrease in the number of compound events per winter  
 405 in ERA5 (-0.19 days per decade; Figure 5a and Table 1). Over the shorter period in common between ERA5  
 406 and MERRA2, compound events have also decreased significantly in ERA5, and at a higher rate (-0.43 days  
 407 per decade). MERRA-2 shows a slightly weaker decrease in compound events (-0.36 days per decade)  
 408 compared to ERA5, which is not significant at the 0.05 level ( $p=0.10$ ). In terms of low wind days, no trend is  
 409 detected in ERA5 over both the longer and shorter periods, and both reanalyses agree on the absence of a  
 410 trend. Conversely, cold days have significantly decreased over the longer period in both the ERA5 reanalysis  
 411 and the E-OBS observations, and at a similar rate of -0.72 and -0.78 days per decade (respectively; Figure 5b

a supprimé: green

a supprimé: Data

... [1]

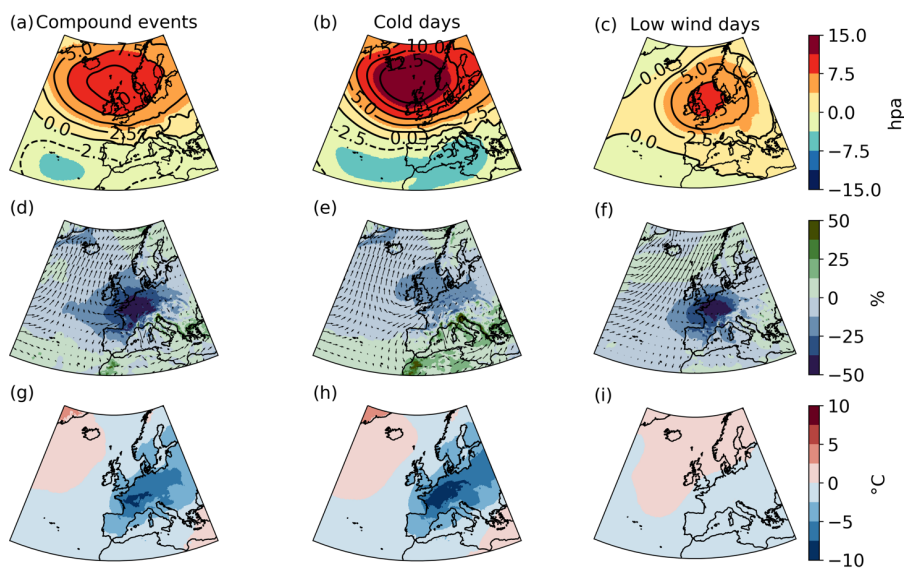
a supprimé: for

a supprimé: its

a supprimé: This might be related to the larger sample of low wind days per winter on average compared to the number of cold days, as defined in this study (section 2.5).

419 and Table 1). Interestingly, over the shorter period in common with ERA5, MERRA2 and EOBS, the  
 420 significance of the negative trend is lost, suggesting that this period might be too short for the influence of  
 421 anthropogenic forcings to emerge from internal variability, contrary to what is observed on the longer period.

### 422 3.2 Role of large-scale circulation.



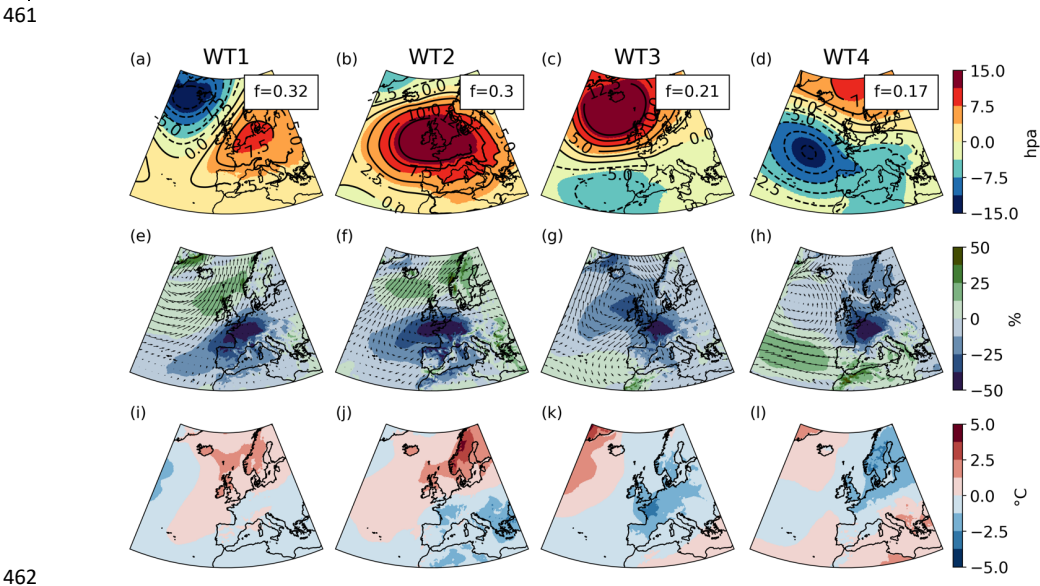
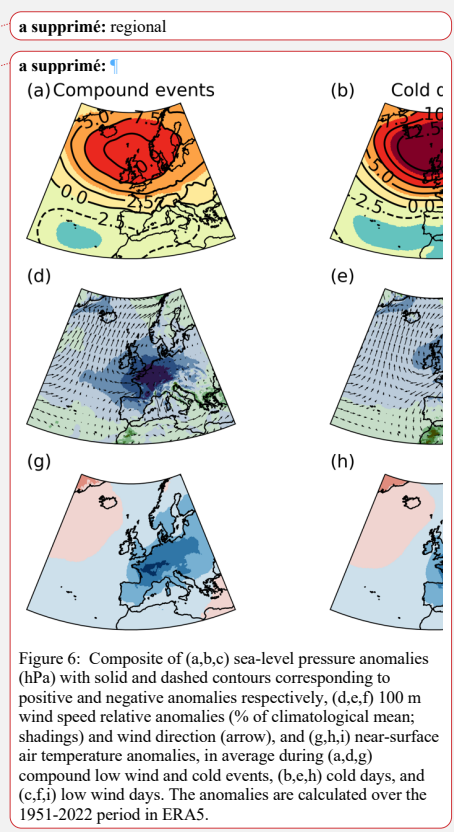
423  
 424 **Figure 6:** Composite of (a,b,c) mean sea-level pressure anomalies (hPa) with solid and dashed  
 425 contours corresponding to positive and negative anomalies respectively, (d,e,f) 100 m wind speed relative  
 426 anomalies, in average during (a,d,g) compound low wind and cold events, (b,e,h) cold days, and  
 427 (c,f,i) low wind days. Relative anomalies for both the temperature and 100-m wind speed are calculated with  
 428 respect to their daily climatology (1950-2022) in ERA5 (smoothed with a 15-day moving average).  
 429

430 On average, the synoptic conditions leading to the occurrence of compound low wind and cold events  
 431 (i.e., compound low wind capacity factor and cold events) are characterized by strong positive mean sea-level  
 432 pressure anomalies over the British Isles and relatively less intense negative anomalies centred on the Azores  
 433 (Figure 6a). Overall, the average large-scale circulation during compound events is very well spatially  
 434 correlated with that of cold days (Figure 6b), but the intensity of the positive anomalies and associated pressure  
 435 dipole are weaker in the case of compound events. The anomalies in mean sea-level pressure are somehow  
 436 different during low wind days compared to compound and cold events. Positive sea level pressure anomalies  
 437 are found further south over the North Sea, with relatively lower intensity, and the negative anomalies over  
 438 the Azores are not as clear (Figure 6c).

439 On average during the compound events defined for the French electricity system solely, negative  
 440 anomalies of wind speed and temperature expand over a wider European domain, comprising Germany and

a supprimé: By definition, during compound low wind and cold events, France experiences calm and cold temperature conditions.  
 a supprimé: the

445 the British Isles, with anomalies up to -40% and -7.5°C, respectively (Figure 6d,g). The negative temperature  
 446 anomalies over France and surrounding countries are slightly weaker during compound events compared to  
 447 cold days (Figure 6g,h). These cold anomalies are induced by a north-easterly flow advecting cold polar air  
 448 towards western Europe. During cold days, and compared to compound events, the negative anomalies in  
 449 wind speed are less intense, the advection of cold air is stronger, and thus colder temperatures are experienced  
 450 over western Europe. During low wind days, negative wind anomalies are found over western Europe, with  
 451 intensities rather similar to those during compound events, along with neutral temperature anomalies (Figure  
 452 6f,i). We find relatively higher similarities in the mean sea-level pressure anomalies between cold days and  
 453 compound events compared to between low wind days and compound events. This can be explained by a more  
 454 extreme threshold used for cold days compared to low wind days in the definition of compound events. Note  
 455 that the sensitivity to thresholds used in the definition of compound events is documented in Supplementary  
 456 Materials. While we find that sea-level pressure anomalies between low wind days and compound events  
 457 compare better when setting a more extreme threshold for low wind days in the compound event definition,  
 458 the main conclusions of this work are generally not sensitive to these thresholds (Figure S3). It is important to  
 459 acknowledge that these average climate conditions might hide a variety of different large-scale atmospheric  
 460 circulations, further explored in the following section using a weather type analysis.



464 Figure 7: Composite of (a,b,c,d) sea-level pressure anomalies (hPa) with solid and dashed contours  
 465 corresponding to positive and negative anomalies respectively, (e,f,g,h) 100 m wind speed relative  
 466 anomalies magnitude (% of climatological mean; shadings) and wind direction (arrows), and (i,j,k,l)  
 467 near-surface air temperature anomalies corresponding to the weather types of low wind days (a,e,i) WT1, (b,f,j) WT2, (c,g,k)

480  
481  
482  
483  
484  
485  
486  
487  
488  
489  
490  
491  
492  
493  
494  
495  
496  
497  
498  
499  
500  
501  
502  
503  
504  
505  
506  
507  
508  
509  
510  
511  
512  
513  
514  
515

WT3 and (d,h,l) WT4. The frequency (f) of the weather types is shown in the upper right corner in panels a,b,c,d.

Four weather types are obtained by classifying the mean sea-level pressure during low wind days using the k-means algorithm (see section 2.6). We then assess the distribution of compound low wind and cold events across these four weather types to identify the most favorable synoptic situations leading to the occurrence of these compound events in France, and over western Europe more generally.

The frequency of weather types of low wind days is rather similar, and ranges from 0.17 (WT4) to 0.32 (WT1). While all four weather types are characterized by low wind conditions (by definition), interestingly, they are also associated with cold temperatures in France and they reveal a diversity of large-scale atmospheric conditions (Figure 7):

- WT1 is characterized by positive mean sea-level pressure anomalies over the Netherlands and northern Germany, and negative anomalies over Iceland. The positive anomalies block the entry of the westerlies at the western border of Europe and deviate them further north, thus advecting relatively warm and humid air over northern Europe, and inducing a substantial decrease in wind speed along with cold anomalies in France and western Europe.
- WT2 shares blocking-like characteristics with WT1, but with more intense positive mean sea level pressure anomalies and over a wider domain extending further west, pushing the negative mean sea-level pressure anomalies further to the north-western corner of the domain. As in WT1, the westerlies are derived north of Europe, inducing a similar dipole of warmer temperatures in the north and colder temperatures under the positive pressure anomalies. In France and southern Europe in general, and compared to WT1, the negative anomalies in wind and temperature are enhanced because of the amplified positive pressure anomalies.
- WT3 shows pronounced positive mean sea-level pressure anomalies over Iceland and negative anomalies west of Portugal. This WT resembles the most to the average atmospheric conditions during compound events (Figure 6a). The dipole of pressure anomalies results in a strong north to north-easterly flow advecting cold air masses from Scandinavia to France. This weather type is associated with the coldest temperatures over France compared to the other weather types, and generally over the entire European domain that also experiences low wind conditions.
- WT4 is rather different from WT1, WT2 and WT3 as it is characterized by substantial negative mean sea-level pressure anomalies in the eastern Atlantic and positive anomalies over the Norwegian Sea. These pressure anomalies induce low wind conditions in France and generally the northern part of Europe, and a reinforcement of the westerlies in the southern part of the domain. This is associated with colder temperatures in the north, including the northern part of France, and positive or low temperature anomalies in south-western Europe.

a supprimé: The anomalies are calculated over the 1951-2022 period in ERA5.

a supprimé: The four weather types obtained with the k-means algorithm (section 2.6) help to identify the most favorable synoptic situations leading to the occurrence of compound low wind and cold events in France, and over western Europe more generally.

a supprimé: and

a supprimé: (by definition)

a supprimé: ,

a supprimé: regional

a supprimé: SLP

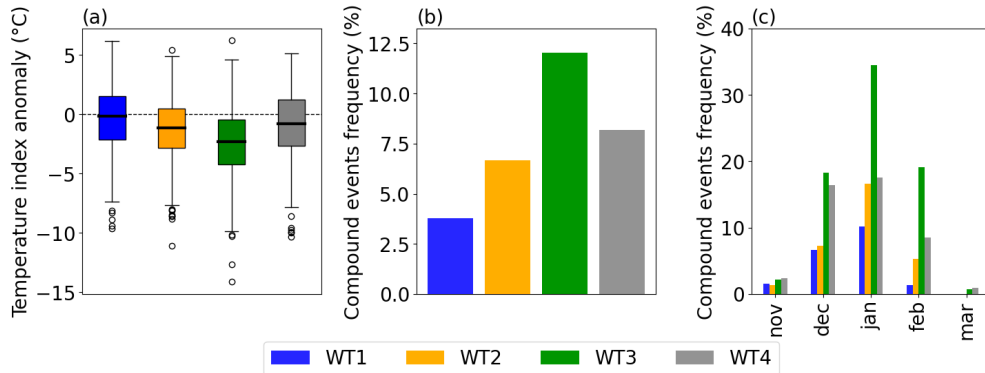


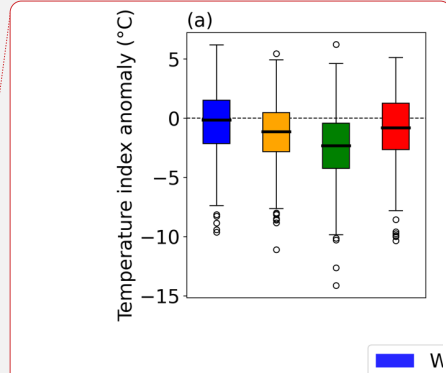
Figure 8: (a) Distribution of temperature index anomalies for each weather type of low wind days (WT; as defined in Figure 7 and indicated in inserted legend); (b) Frequency of compound low wind and cold events for each weather type of low wind days (in % of the weather type size). (c) Frequency of compound low wind and cold events for each weather type of low wind days and each individual winter month (in % of the weather type size for a given month). Temperature index anomalies are calculated with respect to the daily climatology (1950-2022) in ERA5 (smoothed with a 15-day moving average).

The temperature index shows a substantial variability within each weather type of low wind days (Figure 8a). All weather types present very cold days, with anomalies as large as  $-10^{\circ}\text{C}$  for WT1 and WT4, and  $-14^{\circ}\text{C}$  for WT3. WT3 is the coldest weather type and WT1 is relatively warmer than the others over France. The frequency of compound events when a particular weather type occurs varies from 4% in WT1 to 12% in WT3, while WT2 and WT4 present similar values of 7% and 8% (Figure 8b). Importantly, the weather type WT3, which is associated with the highest frequency of compound events, also leads to negative anomalies in wind speed and temperature across the majority of Europe (Figure 7c,g,k). This suggests that this weather type might challenge the electricity system on the larger scale of western Europe.

The frequency of compound events in each weather type shows important monthly variations. For all weather types, the frequency of compound events is higher in January, when climatological temperature reaches the lowest values, compared to other months (Figure 8c). This is especially the case for WT3, for which nearly 35% of days occurring in January are compound events. This important role of the temperature seasonality within each weather type is consistent with the overall seasonality of compound events discussed in section 3.1.

WT1	WT2	WT3	WT4
0.0 (0.78)	0.56 (0.16)	-0.27 (0.29)	<b>-0.59 (0.01)</b>

Table 2: Trend (slope in days/decade) and associated p-value in the frequency of each weather type of low wind days (WT; as defined in Figure 7) in winter over the 1951-2022 period in ERA5. The slope is calculated with the Theil-Sen estimator and the p-value is calculated with the Mann-Kendall test. Significant trends with  $p < 0.05$  are shown in bold.



a supprimé: The anomalies and frequencies are calculated over the 1951-2022 period in ERA5.

a supprimé: intra-type and inter-type

a supprimé: overall, with the lowest median of the temperature index...

a supprimé: Yet, all weather types present very cold days, with anomalies as large as  $-10^{\circ}\text{C}$  for WT1 and WT4, and  $-14^{\circ}\text{C}$  for WT3. ...

a supprimé: It

a supprimé: a

a supprimé: than just in France

a supprimé: s

a supprimé: WT1

... [2]

570  
571  
572  
573  
574  
575  
576  
577  
578  
579  
580  
581  
582

Only the frequency of WT4 shows a significant negative trend over the 1951-2022 period (-0.59 day per decade,  $p=0.01$ ; Table 2). The frequency of WT2 is found to increase (+0.56 day per decade), whereas WT3, which is associated with the highest frequency of compound events, decreases (-0.27 day per decade) over the observed period. These trends for both WT2 and WT3 are however not significant.

To estimate the contribution of the trends in weather type frequencies on the overall evolution of compound events, trends values are multiplied by the frequency of compound events for each corresponding weather type, as done in Horton et al. (2015). Then, the respective contributions from all four weather types are added to estimate the overall influence of the trends in weather type frequencies. This leads to a weak decrease in the frequency of compound events of 20%. This analysis suggests a relatively minor influence of large-scale circulation on the trend of compound events. However, due to significant intra-type variability, a change in the frequency of a few weather types may not capture the full range of circulation changes.

a supprimé: T  
a supprimé: the  
a supprimé: the  
a supprimé: Overall  
a supprimé: , the trends in weather type frequencies lead to  
a supprimé: simple

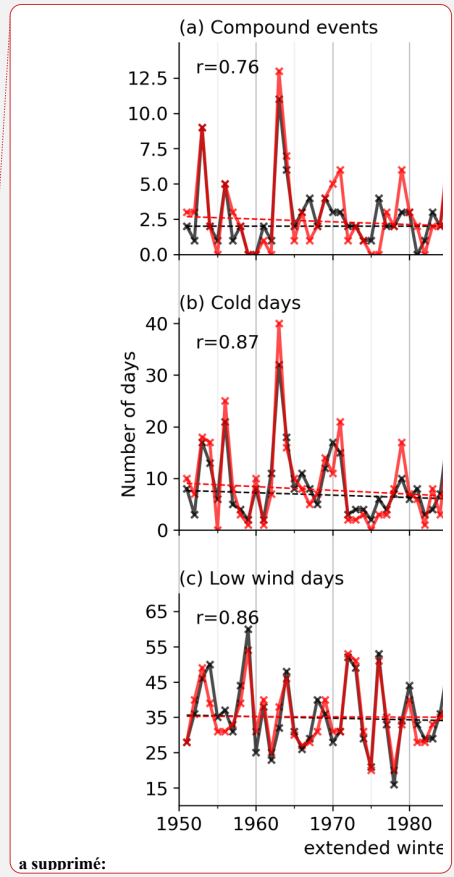
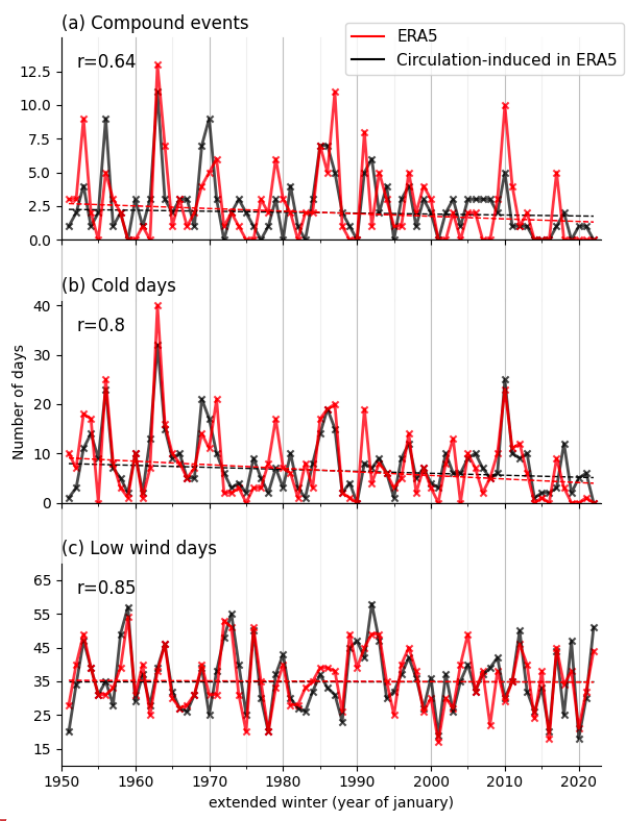


Figure 9: Interannual evolution of the number of (a) circulation-induced compound low wind and cold events, (b) cold days, and (c) low wind days in winter over the 1951-2022 period in ERA5. For each event, the value of the correlation coefficient between the inter-annual evolution and its respective circulation-induced

a supprimé:



evolution is shown in the upper left. Dashed lines show the linear trend (calculated using the Theil-Sen estimator; see Table 3 for the slope value and associated p-value).

	Compound events	Cold days	Low wind days
ERA5	<b>-0.19 (0.02)</b>	<b>-0.72 (0.02)</b>	-0.08 (0.59)
Circulation-induced in ERA5	<b>-0.14 (0.04)</b>	-0.40 (0.14)	-0.21 (0.75)

Table 3: (first row) Trend (slope in days/decade, and associated p-value) in the frequency of low wind days, cold days, and compound low wind and cold events in winter over the period 1951-2022 in ERA5 (first row; same trend estimates as in Table 1) and in their respective circulation-induced events (second row; section 2.7). The slope is calculated with the Theil-Sen estimator and the p-value is calculated with the Mann-Kendall test. Significant trends with  $p < 0.05$  are shown in bold.

The dynamical adjustment approach described in section 2.7 is now used to better quantify the role of the large-scale circulation in the evolution of compound low wind and cold events. The interannual variability in the occurrence of both cold days and low wind days is very well explained by the large-scale circulation (correlations with the corresponding circulation-induced event of 0.80 and 0.85, respectively; Figure 9a,b). Therefore, the interannual variability in the number of compound events is also well explained by the large-scale circulation (correlations with the circulation-induced compound events of  $r=0.64$ , Figure 9a). Extreme winters in terms of compound events such as 1963, 1987, or 2010 are due to a large extent to the atmospheric circulation. Interestingly, circulation-induced cold days substantially decrease (-0.40 days per decade; Table 3), although the p-value does not reach the 0.05 significance level (p-value=0.14). Large-scale circulation may therefore have contributed to more than 50% of the decline in cold days occurrence (-0.72 days per decade, Table 3) observed between 1951 and 2022, suggesting that anthropogenic forcing may not be the only driver of this trend. Similarly, circulation-induced compound events show a decrease (-0.14 days per decade, Table 3) over the 1951-2022 period (p-value=0.04). However, both the trend significance and the magnitude of the slope are sensitive to the parameters used in the dynamical adjustment (not shown). Thus, the robustness is too weak and prevents us from drawing conclusions on the role of the large-scale circulation on the decrease in compound events. Finally, there is no significant trend in the circulation-induced low wind days.

#### 4. Discussion and conclusions

In the context of the energy transition, compound low wind capacity factor and cold events could present a stronger threat for the adequacy between the demand and supply in electricity in France. Therefore, it is crucial to characterize these climate compound events and to better understand how their frequency has changed in the past to better anticipate how they could evolve in the coming decades.

a supprimé: ... [3]

a supprimé: Table 3: (first row) Trend (slope in days/decade, and associated p-value) in the frequency of low wind days, cold days, and compound low wind and cold events in winter over the period 1951-2022 in ERA5 (first row; same trend estimates as in Table 1) and in their respective dynamic component (second row; section 2.7). The slope is calculated with the Theil-Sen estimator and the p-value is calculated with the Mann-Kendall test. Significant trends with  $p < 0.05$  are highlighted with grey shading.

a supprimé: dynamic component

a supprimé: 7

a supprimé: 6

a supprimé: corresponding dynamic component

a supprimé: 76

a supprimé: The dynamic component of compound events shows no significant trend over the 1951-2022 period. This suggests that the large-scale circulation has not played an important role in the observed decrease in the occurrence of compound events. Interestingly, the dynamic component of cold days substantially decreases (-0.47 days per winter; Table 3), although the p-value does not reach the 0.05 significance level (p-value=0.08). Large-scale circulation may therefore have contributed to more than 50% of the decline in cold days occurrence (-0.87 days per winter, Table 3) observed between 1951 and 2022, suggesting that anthropogenic forcing may not be the only driver of this trend. Finally, there is no significant trend in the dynamic component of low wind days.

655 Compound events are defined with ERA5 data over the 1950-2022 period using a wind capacity factor  
656 index, and a temperature index that captures the current sensitivity of the electricity demand in France to  
657 temperature. As compound events mainly occur between November and March, our analyses focus on this  
658 period.

a supprimé: low wind and cold

a supprimé: low wind and cold

659  
660 Compound events are quite rare (2 days per winter on average), with a peak occurrence in January.  
661 They are generally short-lived, with a mean duration of 2 consecutive days although they can last up to 7  
662 consecutive days. There are large interannual differences in the number of compound events, from 0 to 13  
663 days per winter.

a supprimé: 13

664 Over the observational record, we find a statistically significant decrease in compound events  
665 frequency (-0.19 day per decade) that tends to have amplified over the last four decades. This decrease is likely  
666 driven by the significant negative trend in cold days, while the frequency in low wind days shows no  
667 significant trend. Overall, these results suggest a decrease in climate-related risks for the adequacy between  
668 electricity demand and supply related to compound events over the observed period, considering the current  
669 electricity system.

a supprimé: low wind and cold

670 The role of the atmospheric circulation in the occurrence of compound events is assessed using a set  
671 of four weather types derived with the unsupervised k-means classification technique applied to low wind  
672 days. The frequency of compound events in each weather type ranges from 4% to 12%. This reveals a diversity  
673 of large-scale atmospheric circulations that can lead to the occurrence of compound events in France. The  
674 weather type associated with the highest compound events frequency (WT3) presents pronounced positive  
675 sea-level pressure anomalies over Iceland and negative anomalies west of Portugal. This weather type leads  
676 to negative anomalies of wind speed and temperature throughout Europe, which might pose challenges to the  
677 electricity system on a larger scale than just in France. Other studies focusing on compound low wind and  
678 cold events at the scale of Europe also highlight the role of large-scale circulation in compound event  
679 occurrence. Bloomfield (2019) and Tedesco (2023) find that pronounced positive mean sea-level pressure  
680 anomalies over Northern Europe and negative anomalies over the Azores lead to a large number of compound  
681 events in Central and Western Europe, and this circulation pattern projects well onto the weather type WT3 of  
682 this study. Similarly, Otero (2022) finds that a particular weather type (called Greenland blocking), which is  
683 similar to our weather type WT3, increases the probability of compound events in Europe. This is also true  
684 for a second weather type (called European blocking) that projects relatively well onto our weather type WT2.  
685 Hence, in this study, we identify large-scale circulation patterns associated with compound events in France  
686 that compare broadly with previous findings focused over Europe. There are slight discrepancies in the  
687 location of the positive and/or negative anomalies, and these might be partly explained by differences in the  
688 particular domain of interest. Other methodological differences such as weather types calculation or definition  
689 of compound events might also explain some differences.

a supprimé: regional

Overall, we find that the large-scale atmospheric circulation contributes substantially to the occurrence of compound events and explains an important part of their interannual variability. Interestingly, the large-scale atmospheric circulation shows a contribution of approximately 50% of the observed decrease in cold days over the 1951-2022 period in ERA5. Similarly, Deser and Phillips (2023) found that large-scale circulation contributes to a third of the mean winter temperature trend in Europe over the last decades. Assuming that observed changes in the large-scale circulation are mainly driven by internal climate variability (Shepherd, 2014), these results suggest that, over the last few decades, climate variability likely reinforced the long-term decline in cold events in response to warming. This may not continue in the near future, potentially leading to a temporary increase in the occurrence of cold events. Finally, we cannot conclude on the role of large-scale circulation in the decrease of compound events as our methodology exhibits sensitivity to its parameters.

In this study, compound low wind capacity factor and cold events are identified using a straightforward approach that consists of identifying cold days and low wind capacity factor days independently. This has the advantage of allowing the assessment of the relative contribution of cold days and low wind capacity factor days to the decrease in compound events. Another approach consists in identifying compound events as days with high residual load (i.e., electricity demand minus wind power production), i.e., days that need important availability of other power sources than wind power, such as hydro-electricity or nuclear generation (Bloomfield et al., 2020a). Such approach could help to test the sensitivity of compound events to different power system scenarios (e.g., with different wind power installed capacity).

With the anticipated rapid growth of onshore and offshore wind farms, the impact of low wind conditions on power system risks is likely to increase and to become a greater threat alongside cold temperature conditions. As climate change reduces the frequency of cold events (Seneviratne, 2021), future risks to the French power system may be more evenly spread throughout the winter season, rather than being concentrated primarily in January and February as it is currently (RTE, 2023, §6.2.5.3). In addition, changes in electricity demand patterns are also anticipated. During summer, increased electricity demand is expected due to higher use of air conditioning in France. However, the risks for the French power system during summer are expected to be limited thanks to higher solar power production and power system flexibilities (RTE, 2023, §6.2.5.3). How the risk on the adequacy between electricity generation and demand associated with compound events will evolve in the next few decades is therefore multifaceted, depending on future levels of installed wind power capacity, changes in demand patterns, and climate change. We plan to address some of these questions in future work using climate projections from the latest Couple Model Intercomparison Project Phase 6.

Future risks for the electricity system will also depend on the amount of electricity that can be stored to modulate the variability of renewable energy production. In this context, long-lasting compound low wind and cold events at the European scale will be of particular relevance. The study of such long events impacting

a supprimé: regional

a supprimé: significantly

a supprimé: Interestingly, the regional atmospheric circulation shows no significant contribution in the observed decrease in compound events over the 1951-2022 period in ERA5

a supprimé: In the case of cold days, however, the large-scale circulation might contribute to approximately 50% of their observed decrease.

a supprimé: As large-scale circulation variability is likely to be largely internal in origin, this result may have implications for near-term projections.

a supprimé: With the anticipated rapid increase in onshore and offshore wind farms, the impact of low wind conditions on French electricity production is expected to increase. Conversely, the impact of cold events on French electricity demand is expected to decrease due to climate change. The question of how the risk on the adequacy between electricity production and demand associated with compound events will evolve in the next few decades is therefore multifaceted, depending on both the future level of installed wind power capacity and climate change. We plan to address this question in future work using climate projections from the latest Couple Model Intercomparison Project Phase 6.

755 a large domain requires a large sample. The use of the ERA5 reanalysis in this context is therefore not  
756 appropriate. An interesting option is to use state of the art Earth System Models, which provide large  
757 ensembles of simulations that enable identifying a higher number of long and high impact compound events  
758 (Bevacqua et al., 2023).

759 How the occurrence of compound events will continue to evolve in a changing climate is also a crucial  
760 question in the context of the energy transition. This study lays a methodological groundwork for addressing  
761 this question. It can also serve as a reference for the evaluation and selection of climate models that could then  
762 be used to assess the projections in compound events. In particular, our findings highlight the important role  
763 of the **large-scale** atmospheric circulation in driving compound low wind and cold events in winter in France,  
764 and this contribution is therefore a relevant metric for model evaluation in this context.

a supprimé: regional

## 766 **Statements & Declarations**

767 **Fundings.** This study is part of a PhD project funded by Réseau de Transport d'Electricité (RTE).

768 **Competing Interests.** The authors declare they have no conflict of interest.

769 **Author contributions.** All authors contributed to the study conception and design. Data collection and  
770 analysis were performed by FC, MB and JB. All authors contributed to the interpretation of the results. The  
771 first draft of the manuscript was written by FC, MB and JB and all authors commented on previous versions  
772 of the manuscript. All authors read and approved the final manuscript.

773 **Data availability.** The ERA5 reanalysis data is available on the Copernicus Data Store (CDS) at  
774 <https://cds.climate.copernicus.eu/cdsapp#!/dataset/reanalysis-era5-single-levels?tab=overview> (Hersbach et  
775 al., 2020). The MERRA-2 reanalysis data is available from NASA at  
776 [https://disc.gsfc.nasa.gov/datasets/M2TINXLND\\_5.12.4/summary](https://disc.gsfc.nasa.gov/datasets/M2TINXLND_5.12.4/summary) (Gelaro et al., 2017). The E-OBS gridded  
777 in situ observation datasets is provided by the European Climate Assessment & Dataset and available at:  
778 <https://www.ecad.eu/download/ensembles/download.php>.

779

780

782 **References**

- 783 [Añel, J., Fernández-González, M., Labandeira, X., López-Otero, X., and De La Torre, L.: Impact of Cold](#)  
784 [Waves and Heat Waves on the Energy Production Sector, \*Atmosphere\*, 8, 209,](#)  
785 <https://doi.org/10.3390/atmos8110209>, 2017.  
786
- 787 Bevacqua, E., Suarez-Gutierrez, L., Jézéquel, A., Lehner, F., Vrac, M., Yiou, P., and Zscheischler, J.:  
788 Advancing research on compound weather and climate events via large ensemble model simulations, *Nat*  
789 *Commun*, 14, 2145, <https://doi.org/10.1038/s41467-023-37847-5>, 2023.
- 790
- 791 Bloomfield, H. C., Brayshaw, D. J., and Charlton-Perez, A. J.: Characterizing the winter meteorological  
792 drivers of the European electricity system using targeted circulation types, *Meteorol Appl*, 27,  
793 <https://doi.org/10.1002/met.1858>, 2020a.
- 794
- 795 Bloomfield, H. C., Brayshaw, D. J., and Charlton-Perez, A. J.: Characterizing the winter meteorological  
796 drivers of the European electricity system using targeted circulation types, *Meteorol Appl*, 27,  
797 <https://doi.org/10.1002/met.1858>, 2020b.
- 798
- 799 Bloomfield, H. C., Brayshaw, D. J., Deakin, M., and Greenwood, D.: Hourly historical and near-future weather  
800 and climate variables for energy system modelling, *Earth Syst. Sci. Data*, 14, 2749–2766,  
801 <https://doi.org/10.5194/essd-14-2749-2022>, 2022.
- 802
- 803 Boé, J., Mass, A., and Deman, J.: A simple hybrid statistical–dynamical downscaling method for emulating  
804 regional climate models over Western Europe. Evaluation, application, and role of added value?, *Clim Dyn*,  
805 61, 271–294, <https://doi.org/10.1007/s00382-022-06552-2>, 2023.
- 806
- 807 Cassou, C.: Intraseasonal interaction between the Madden–Julian Oscillation and the North Atlantic  
808 Oscillation, *Nature*, 455, 523–527, <https://doi.org/10.1038/nature07286>, 2008.
- 809
- 810 Cattiaux, J., Vautard, R., Cassou, C., Yiou, P., Masson-Delmotte, V., and Codron, F.: Winter 2010 in Europe:  
811 A cold extreme in a warming climate, *Geophysical Research Letters*, 37, 2010GL044613,  
812 <https://doi.org/10.1029/2010GL044613>, 2010.
- 813
- 814 Cornes, R. C., Van Der Schrier, G., Van Den Besselaar, E. J. M., and Jones, P. D.: An Ensemble Version of  
815 the E-OBS Temperature and Precipitation Data Sets, *JGR Atmospheres*, 123, 9391–9409,  
816 <https://doi.org/10.1029/2017JD028200>, 2018.
- 817
- 818 Deser, C. and Phillips, A. S.: A range of outcomes: the combined effects of internal variability and  
819 anthropogenic forcing on regional climate trends over Europe, *Nonlin. Processes Geophys.*, 30, 63–84,  
820 <https://doi.org/10.5194/npg-30-63-2023>, 2023.
- 821
- 822 Deser, C., Terray, L., and Phillips, A. S.: Forced and Internal Components of Winter Air Temperature Trends  
823 over North America during the past 50 Years: Mechanisms and Implications\*, *Journal of Climate*, 29, 2237–  
824 2258, <https://doi.org/10.1175/JCLI-D-15-0304.1>, 2016.
- 825
- 826 Falkena, S. K. J., de Wiljes, J., Weisheimer, A., and Shepherd, T. G.: Revisiting the Identification of  
827 Wintertime Atmospheric Circulation Regimes in the Euro-Atlantic Sector, *Quart J Royal Meteorol Soc*, 146,  
828 2801–2814, <https://doi.org/10.1002/qj.3818>, 2020.
- 829
- 830 Gelaro, R., McCarty, W., Suárez, M. J., Todling, R., Molod, A., Takacs, L., Randles, C. A., Darmenov, A.,  
831 Bosilovich, M. G., Reichle, R., Wargan, K., Coy, L., Cullather, R., Draper, C., Akella, S., Buchard, V., Conaty,  
832 A., Da Silva, A. M., Gu, W., Kim, G.-K., Koster, R., Lucchesi, R., Merkova, D., Nielsen, J. E., Partyka, G.,  
833 Pawson, S., Putman, W., Rienecker, M., Schubert, S. D., Sienkiewicz, M., and Zhao, B.: The Modern-Era  
834 Retrospective Analysis for Research and Applications, Version 2 (MERRA-2), *J. Climate*, 30, 5419–5454,

835 <https://doi.org/10.1175/JCLI-D-16-0758.1>, 2017.  
836  
837 Grams, C. M., Beerli, R., Pfenninger, S., Staffell, I., and Wernli, H.: Balancing Europe's wind-power output  
838 through spatial deployment informed by weather regimes, *Nature Clim Change*, 7, 557–562,  
839 <https://doi.org/10.1038/nclimate3338>, 2017.  
840  
841 Hersbach, H., Bell, B., Berrisford, P., Hirahara, S., Horányi, A., Muñoz-Sabater, J., Nicolas, J., Peubey, C.,  
842 Radu, R., Schepers, D., Simmons, A., Soci, C., Abdalla, S., Abellan, X., Balsamo, G., Bechtold, P., Biavati,  
843 G., Bidlot, J., Bonavita, M., Chiara, G., Dahlgren, P., Dee, D., Diamantakis, M., Dragani, R., Flemming, J.,  
844 Forbes, R., Fuentes, M., Geer, A., Haimberger, L., Healy, S., Hogan, R. J., Hólm, E., Janisková, M., Keeley,  
845 S., Laloyaux, P., Lopez, P., Lupu, C., Radnoti, G., Rosnay, P., Rozum, I., Vamborg, F., Villaume, S., and  
846 Thépaut, J.: The ERA5 global reanalysis, *Q.J.R. Meteorol. Soc.*, 146, 1999–2049,  
847 <https://doi.org/10.1002/qj.3803>, 2020.  
848  
849 Hirschi, J. J. -M. and Sinha, B.: Negative NAO and cold Eurasian winters: how exceptional was the winter of  
850 1962/1963?, *Weather*, 62, 43–48, <https://doi.org/10.1002/wea.34>, 2007.  
851  
852 Horton, D. E., Johnson, N. C., Singh, D., Swain, D. L., Rajaratnam, B., and Diffenbaugh, N. S.: Contribution  
853 of changes in atmospheric circulation patterns to extreme temperature trends, *Nature*, 522, 465–469,  
854 <https://doi.org/10.1038/nature14550>, 2015.  
855  
856 Jourdir, B.: Evaluation of ERA5, MERRA-2, COSMO-REA6, NEWA and AROME to simulate wind power  
857 production over France, *Adv. Sci. Res.*, 17, 63–77, <https://doi.org/10.5194/asr-17-63-2020>, 2020.  
858 Lorenz, E. N.: Atmospheric Predictability as Revealed by Naturally Occurring Analogues, *Journal of*  
859 *Atmospheric Sciences*, 26, 636–646, [https://doi.org/10.1175/1520-0469\(1969\)26<636:APARBN>2.0.CO;2](https://doi.org/10.1175/1520-0469(1969)26<636:APARBN>2.0.CO;2),  
860 1969.  
861  
862 Manwell, J. F.: *Wind Energy Explained: Theory, Design and Application*, n.d.  
863  
864 Najac, J., Boé, J., and Terray, L.: A multi-model ensemble approach for assessment of climate change impact  
865 on surface winds in France, *Clim Dyn*, 32, 615–634, <https://doi.org/10.1007/s00382-008-0440-4>, 2009.  
866  
867 Olauson, J.: ERA5: The new champion of wind power modelling?, *Renewable Energy*, 126, 322–331,  
868 <https://doi.org/10.1016/j.renene.2018.03.056>, 2018.  
869  
870 Otero, N., Martius, O., Allen, S., Bloomfield, H., and Schaeffli, B.: A copula-based assessment of renewable  
871 energy droughts across Europe, *Renewable Energy*, 201, 667–677,  
872 <https://doi.org/10.1016/j.renene.2022.10.091>, 2022a.  
873  
874 Otero, N., Martius, O., Allen, S., Bloomfield, H., and Schaeffli, B.: Characterizing renewable energy  
875 compound events across Europe using a logistic regression-based approach, *Meteorological Applications*, 29,  
876 <https://doi.org/10.1002/met.2089>, 2022b.  
877  
878 Plaut, G. and Simonnet, E.: Large-scale circulation classification, weather regimes, and local climate over  
879 France, the Alps and Western Europe, *Clim. Res.*, 17, 303–324, <https://doi.org/10.3354/cr017303>, 2001.  
880 Rapella, L., Faranda, D., Gaetani, M., Drobinski, P., and Ginesta, M.: Climate change on extreme winds  
881 already affects off-shore wind power availability in Europe, *Environ. Res. Lett.*, 18, 034040,  
882 <https://doi.org/10.1088/1748-9326/acbdb2>, 2023.  
883  
884 Ravestein, P., Van Der Schrier, G., Haarsma, R., Scheele, R., and Van Den Broek, M.: Vulnerability of  
885 European intermittent renewable energy supply to climate change and climate variability, *Renewable and*  
886 *Sustainable Energy Reviews*, 97, 497–508, <https://doi.org/10.1016/j.rser.2018.08.057>, 2018.  
887 Raynaud, D., Hingray, B., François, B., and Creutin, J. D.: Energy droughts from variable renewable energy  
888 sources in European climates, *Renewable Energy*, 125, 578–589,

889 <https://doi.org/10.1016/j.renene.2018.02.130>, 2018.

890 RTE (Réseau de transport d'électricité), Futurs énergétiques 2050. Les scénarios de mix de production à  
891 l'étude permettant d'atteindre la neutralité carbone à l'horizon 2050, octobre 2021.

892 RTE (Réseau de transport d'électricité). Bilan prévisionnel, édition 2023. Futurs énergétiques 2050. 2023-  
893 2035 : première étape vers la neutralité carbone.

894 Saffioti, C., Fischer, E. M., Scherrer, S. C., and Knutti, R.: Reconciling observed and modeled temperature  
895 and precipitation trends over Europe by adjusting for circulation variability, *Geophysical Research Letters*,  
896 43, 8189–8198, <https://doi.org/10.1002/2016GL069802>, 2016.

897  
898 Seneviratne, S.I., X. Zhang, M. Adnan, W. Badi, C. Dereczynski, A. Di Luca, S. Ghosh, I. Iskandar, J. Kossin,  
899 S. Lewis, F. Otto, I. Pinto, M. Satoh, S.M. Vicente-Serrano, M. Wehner, and B. Zhou: *Weather and Climate*  
900 *Extreme Events in a Changing Climate.*, 1st ed., Cambridge University Press,  
901 <https://doi.org/10.1017/9781009157896>, 2021.

902  
903 [Shepherd, T. G.: Atmospheric circulation as a source of uncertainty in climate change projections, \*Nature\*  
904 \*Geosci.\*, 7, 703–708, <https://doi.org/10.1038/ngeo2253>, 2014.](https://doi.org/10.1038/ngeo2253)

905  
906 Sippel, S., Meinshausen, N., Merrifield, A., Lehner, F., Pendergrass, A. G., Fischer, E., and Knutti, R.:  
907 Uncovering the Forced Climate Response from a Single Ensemble Member Using Statistical Learning, *Journal*  
908 *of Climate*, 32, 5677–5699, <https://doi.org/10.1175/JCLI-D-18-0882.1>, 2019.

909  
910 Sippel, S., Fischer, E. M., Scherrer, S. C., Meinshausen, N., and Knutti, R.: Late 1980s abrupt cold season  
911 temperature change in Europe consistent with circulation variability and long-term warming, *Environ. Res.*  
912 *Lett.*, 15, 094056, <https://doi.org/10.1088/1748-9326/ab86f2>, 2020.

913  
914 Staffell, I. and Pfenninger, S.: Using bias-corrected reanalysis to simulate current and future wind power  
915 output, *Energy*, 114, 1224–1239, <https://doi.org/10.1016/j.energy.2016.08.068>, 2016.

916  
917 Tedesco, P., Lenkoski, A., Bloomfield, H. C., and Sillmann, J.: Gaussian copula modeling of extreme cold  
918 and weak-wind events over Europe conditioned on winter weather regimes, *Environ. Res. Lett.*, 18, 034008,  
919 <https://doi.org/10.1088/1748-9326/acb6aa>, 2023.

920  
921 Terray, L.: A dynamical adjustment perspective on extreme event attribution, *Weather Clim. Dynam.*, 2, 971–  
922 989, <https://doi.org/10.5194/wcd-2-971-2021>, 2021.

923  
924 Thornton, H. E., Scaife, A. A., Hoskins, B. J., and Brayshaw, D. J.: The relationship between wind power,  
925 electricity demand and winter weather patterns in Great Britain, *Environ. Res. Lett.*, 12, 064017,  
926 <https://doi.org/10.1088/1748-9326/aa69c6>, 2017.

927  
928 Van Den Dool, H. M.: Searching for analogues, how long must we wait?, *Tellus A*, 46, 314–324,  
929 <https://doi.org/10.1034/j.1600-0870.1994.t01-2-00006.x>, 1994.

930  
931 Van Oldenborgh, G. J., Mitchell-Larson, E., Vecchi, G. A., De Vries, H., Vautard, R., and Otto, F.: Cold  
932 waves are getting milder in the northern midlatitudes, *Environ. Res. Lett.*, 14, 114004,  
933 <https://doi.org/10.1088/1748-9326/ab4867>, 2019.

934  
935 van der Wiel, K., Stoop, L. P., van Zuijlen, B. R. H., Blackport, R., van den Broek, M. A., and Selten, F. M.:  
936 Meteorological conditions leading to extreme low variable renewable energy production and extreme high  
937 energy shortfall, *Renewable and Sustainable Energy Reviews*, 111, 261–275,  
938 <https://doi.org/10.1016/j.rser.2019.04.065>, 2019a.

939  
940

a supprimé: Réseau de Transport d'électricité (RTE): Bilan prévisionnel 2023-2035, 2023.

a supprimé: Réseau de Transport d'électricité (RTE): Futurs Énergétiques 2050 - chapitre 8 (le climat), 2022.

945 van der Wiel, K., Bloomfield, H. C., Lee, R. W., Stoop, L. P., Blackport, R., Screen, J. A., and Selten, F. M.:  
946 The influence of weather regimes on European renewable energy production and demand, *Environ. Res. Lett.*,  
947 14, 094010, <https://doi.org/10.1088/1748-9326/ab38d3>, 2019b.

948  
949 Zscheischler, J., Martius, O., Westra, S., Bevacqua, E., Raymond, C., Horton, R. M., van den Hurk, B.,  
950 AghaKouchak, A., Jézéquel, A., Mahecha, M. D., Maraun, D., Ramos, A. M., Ridder, N. N., Thiery, W., and  
951 Vignotto, E.: A typology of compound weather and climate events, *Nat Rev Earth Environ*, 1, 333–347,  
952 <https://doi.org/10.1038/s43017-020-0060-z>, 2020.

953